Preparation of Oligomeric Phenolic Compounds (DHPs) from Coniferin and Syringin and Characterization of their Anticancer Properties

Yimin Xie,[a,b,*] Chen Jiang,[a] Xuekuan Chen,[a] Hongfei Wu,[a] and Shuying Bi [a]

Lignin precursors of coniferin and syringin were synthesized and used to prepare guaiacyl-type and guaiacyl-syringyl-type oligomeric compounds (designated here as dehydrogenation polymers DHP-G, DHP-GS) *via* bulk method. The carbon 13 nuclear magnetic resonance spectroscopy (^{13}C-NMR) spectra indicated that both DHPs contained typical lignin substructures. The DHPs were extracted sequentially with petroleum ether, ether, ethanol, and acetone to obtain eight fractions (F_{11} to F_{14} and F_{21} to F_{24}). The 3-(4,5-dimethyl-2-thiazolyl)-2,5-diphenyl-2-H-tetrazolium bromide (MTT) experimental results showed that the growth of cervical cancer cells was inhibited by the two ether-soluble fractions F_{12} and F_{22}, with semi-inhibitory concentration (IC_{50}) values of 81.60 ± 9.30 and 103.24 ± 14.09 μg/mL, respectively. The bioactive compounds in F_{12} and F_{22} were separated by a preparative chromatography method. Ten bioactive compounds (G_1 to G_5 and GS_1 to GS_5) were obtained. Mass spectroscopy analysis revealed the following chemical structures: G_1, β-5 G-type dimer; G_2, (β-5)(β-5) G-type trimer; GS_1, β-5 GS-type dimer; and GS_2, (β-O-4)(β-5) GS-type trimer. The compounds had inhibitory effects on cervical cancer cells. The syringyl aromatic ring decreased the anticancer activity of DHP, and the β-O-4 linkages did not contribute to the anticancer activity. It was also found that the carboxyl groups contributed to the anticancer activity of DHP.

Keywords: Lignin; Oligomer; DHP; Anticancer activity; Structure

Contact information: a: Research Institute of Pulp and Paper Engineering, Hubei University of Technology, 430068, Wuhan, China; b: Hubei Provincial Key Laboratory of Green Materials for Light Industry, Hubei University of Technology, 430068, Wuhan, China;
** Corresponding author: ppymxie@163.com*

INTRODUCTION

Currently, considerable effort is being made to find new applications of lignins in order to add extra value (Vinardell and Mitjans 2017). Cancer incidence is increasing every year. Current treatments include surgery, chemotherapy, radiation therapy, and immunotherapy. Many natural plant extracts can be used as effective anticancer agents, such as vinblastine, etoposide, paclitaxel, bleomycin, and taxanes (Mathi *et al*. 2014). However, the amount of commercial anticancer components in plant extracts, such as paclitaxel and taxanes, is minimal, less than 0.1%. Therefore, the focus of recent research has shifted to the development of new natural anticancer drugs from rich lignin resources (Gomes *et al*. 2003). Plant polyphenols have drawn increasing attention due to their potent antioxidant properties and their marked effects in the prevention of various oxidative stress associated diseases such as cancer. For instance, lignin, flavonoids, phenolic acids, and tannins are compounds possessing one or more aromatic rings with

one or more hydroxyl groups. They are broadly distributed in the plant kingdom and are the most abundant aromatic secondary metabolites of plants (Dai and Mumper 2010).

Over the years, botanists, plant physiologists, phytochemists, and biochemists, as well as organic chemists have studied polyphenols in more detail. Results of such studies have shown the significance of polyphenols not only as major and ubiquitous plant secondary metabolites, but also as compounds that express properties with numerous implications and potential exploitations in various domains of general public and commercial interests (Quideau *et al.* 2011). Many studies have demonstrated plant polyphenols to be a major source of anticancer drugs. This is a large class of compounds with high biological activity. For example, the anticancer activity of lignin, as well as its derivatives, has been verified. Barapatre *et al*. (2016) extracted four physiologically active lignin fractions from acacia wood by pressurized solvent extraction (PSE) and successive solvent extraction (SSE) and found that these extracts had inhibitory effects on breast cancer cells (MCF-7). Its semi-inhibitory concentration (IC_{50}) was less than 15 μg/mL, but there was no obvious inhibitory effect on the growth of normal primary human hepatic stellate cells (HHSteCs). In another example, after ethanol defatting of pine fruit by Sakagami *et al.* (2005), the lignin-carbohydrate complex was collected through hot water and alkaline extraction. This complex had an obvious inhibitory effect on mouse ascitic cancer cells and also enhanced the immune response of mice. According to work of Niedzwiecki *et al*. (2016), polyphenols were able to penetrate human tissues, in particular the intestine and liver, where they were metabolized. Similar to the structure and physical properties of natural polyphenols, the oligomeric DHP may also penetrate the tissues of the human organ.

There are many lignin extraction methods (Obst and Kirk 1988; Jia *et al*. 2013). However, the extracted lignin typically has a large scale of molecular weight and contains a small amount of carbohydrate impurities. An artificial lignin with structure most similar to protolignin in plant can be synthesized by dehydrogenation reaction combined with free radical polymerization catalyzed by laccase or lignin peroxidase. Freudenberg (1952) found that coniferyl alcohol could be polymerized to form a dehydrogenation polymer (DHP) under enzymatic catalysis, with a structure that was similar to natural lignin (Guan *et al*. 1997; McCarthy and Islam 1999). To maintain consistent terminology with other publications, the letters DHP will be used in this paper to mean products of such reactions; however, readers are urged to keep in mind that the reaction products may include dimers and trimers rather than polymers. The degree of polymerization of DHP can be regulated by controlling the concentration of the substrate, the ratio of enzyme, temperature, pH, and reaction time. Therefore, DHP with a low degree of polymerization, simple structure and connection mode, and more functional groups can be obtained, resulting in higher biological activity than that of naturally extracted lignin.

The synthesis of oligolignin has been reported (Ye *et al*. 2016; Chen *et al*. 2018; Xie *et al*. 2019). Chen *et al.* (2018) synthesized DHP with isoeugenol as the precursor, and found that the ether-soluble component had strong antioxidant activity with an IC_{50} of 0.12 g/L. However, most of this work focused on the chemical structure of oligolignin rather than its biological activity and anticancer properties. Therefore, research into the relationship between the oligolignin structure and biological activity is still required.

In this study, in order to synthesize the oligomeric artificial lignin, G-type lignin dehydrogenation polymer (DHP-G) and GS-type lignin dehydrogenation polymer (DHP-GS) were synthesized *via* a bulk method starting with coniferin, or a mixture of coniferin and syringin (1:1, molar ratio) under laccase and β-glucosidase catalysis. The two types

of DHP were extracted by solvents. The inhibitory effect of DHP fractions on the growth of human cervical cancer Hela cells was measured by the 3-(4,5-dimethyl-2-thiazolyl)-2,5-diphenyl-2-H-tetrazolium bromide (MTT) assay. The fractions with higher biological activity were further purified and screened to obtain bioactive compounds, which were structurally identified by atmospheric pressure chemical ionization mass spectrometry (APCI-MS). The anticancer activity of these compounds was determined and the source of biological activity discussed from the analysis of the structure-effect relationship.

EXPERIMENTAL

Materials

Coniferin and syringin (Fig. 1) were synthesized in the laboratory from starting materials vanillin and syringaldehyde (Aladdin, Shanghai, China), respectively, according to the previous methods of Xie Yimin(1991) and Xie *et al*. (1994a). β-Glucosidase was purchased from Sigma Co., Ltd. (Shanghai, China) and laccase (No. 51003) from Novazyme Co., Ltd. (Tianjing, China). All other chemicals were of an analytical grade.

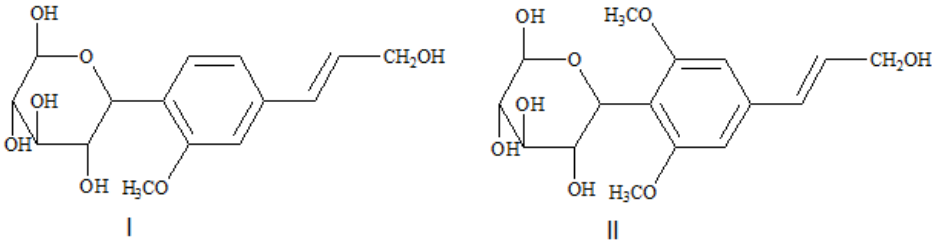

Fig. 1. Chemical structure of the coniferin (I) and syringin (II)

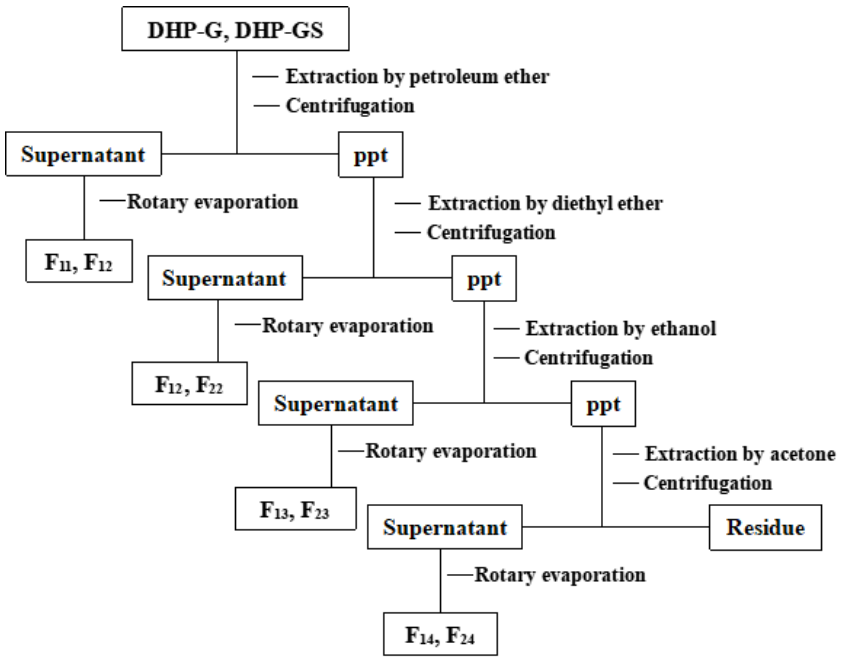

Fig. 2. Fractionation of the DHP-G and DHP-GS by solvents

Synthesis of the DHP-G and DHP-GS

Coniferin (Xie *et al*. 1994b) (9.62 mmol) was dissolved in an acetic acid/sodium acetate buffer solution (pH 4.6, 100 mL). β-Glucosidase (30 mg, 6.4 U/mg) and laccase (2 mL, 1093 IU/mL) were added and the solution mixed with bubbling of sterilized air at 30 °C. The reaction was stopped by addition of hot distilled water (80 °C, 100 mL) after 30 min reaction. After centrifugation (8000 r/min, 8 min), the supernatant was removed and the residue washed thoroughly with water to remove the enzyme and residual lignin precursor, then freeze-dried. The precipitation was extracted with dichloroethane/ethanol (2:1 v/v) mixture, centrifuged at 8000 r/min for 8 min, and the supernatant collected. The solvent was removed *in vacuo* to give the purified DHP-G with 88.3% yield.

The above procedure was also conducted for a mixture of syringin (4.0 mmol) and coniferin (4.0 mmol) as starting material of polymerization, resulting in DHP-GS in 80.9% yield.

Classification of the DHP-G and DHP-GS

As shown in Fig. 2, the DHP-G and DHP-GS were fractionated by the solvent method (Wang *et al*. 2010). The DHPs were extracted with petroleum ether (boiling point 30 to 60 °C), diethyl ether, absolute ethanol, and acetone, sequentially, according to their solubility in the organic solvent. From DHP-G, a petroleum ethersoluble fraction (F_{11}), ether soluble fraction (F_{12}), ethanol soluble fraction (F_{13}), and acetone soluble fraction (F_{14}) were obtained with yields of 2.1%, 26.2%, 31.3%, and 7.8%, respectively. From the DHP-GS, a petroleum ether soluble fraction (F_{21}), ether soluble fraction (F_{22}), ethanol soluble fraction (F_{23}), and acetone soluble fraction (F_{24}) were obtained with yields of 2.5%, 24.3%, 40.8% and 9.7%, respectively.

Methods

^{13}C NMR spectroscopy of DHPs

The DHP-G or DHP-GS (80 mg) was dissolved in dimethyl sulfoxide (DMSO)-d_6 (0.6 mL) and put into a Φ 5 mm NMR tube. The solutions were scanned with a 600-DD2 NMR spectrometer (Agilent Technologies, Santa Clara, CA, USA) at 150.83 MHz to obtain the corresponding ^{13}C-NMR spectrum. The parameters of the instrument were: pulse delay: 2.5000 s, acquisition time: 0.9437 s, and number of scanning time: 6,000.

Molecular weight determination of the DHP fractions

The relative molecular mass was determined by size exclusion chromatography. Each DHP fraction (2 mg) was dissolved in N,N-dimethylformamide (DMF) (2 mL), filtered through a 0.22-μm membrane and injected into a Shimadzu LC 20A gel permeation chromatograph (GPC) (Shimadzu, Kyoto, Japan). The separation column was Shim-pack GPC-803D (300 mm × 8 mm) (Shimadzu, Kyoto, Japan), the mobile phase was DMF, and the flow rate was 0.6 mL/min with a column temperature of 35 °C. The injection volume was 25 μL. Polystyrene was used as standard.

Preparative column chromatography purification of fractions

The fractions with higher anticancer activity were further purified by preparative column chromatography (Büchi C-615, Büchi Lab Equipment, Flawil, Switzerland) according to the following procedure (Tan *et al*. 2011; Xiang 2015). The F_{12} and F_{22} fractions were eluted with acetone/n-hexane (2:3, v/v), acetone/n-hexane (3:2, v/v), and

methanol/chloroform (1:18, v/v), respectively, as shown in Fig. 3. The yields of purified compounds G_1 to G_5 were 39.2%, 28.7%, 15.4%, 8.9%, and 7.8%, respectively. The yields of purified compounds GS_1 to GS_5 were 43.5%, 26.9%, 12.0%, 10.4%, and 7.2%, respectively.

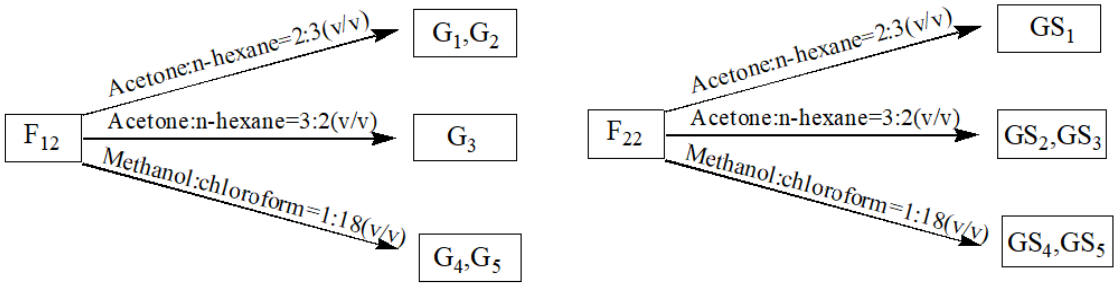

Fig. 3. Column chromatography fractionations of the ether-soluble fractions F_{12} and F_{22}

Determination of anticancer activity of the DHP fractions and purified compounds

Cervical cancer Hela cells (primary cell) in the logarithmic growth phase were adjusted to a concentration of 1×10^4 cells/well in a 96-well flat bottom plate (Mathi *et al*. 2015). The cells were incubated for 24 to 48 h until the cells spread over the bottom. The DHP fractions (100 μL) across a concentration gradient of 10 to 1000 μg/mL were added to each well. After 24 h incubation, 3-(4,5-dimethyl-2-thiazolyl)-2,5-diphenyl-2-H-tetrazolium bromide (MTT) solution (5 mg/mL, 20 μL) was added to each well (Van *et al*. 2011). After 4 h, 150 μL of DMSO was added to each well and the plate was shaken for 10 min on a shaker to fully dissolve the crystals. Finally, the absorbance of each well at 490 nm was measured on a microplate reader (BioTek Instruments Inc., Winooski, VT, USA). The relationship between the concentration of each sample and the inhibition rate was plotted and the IC_{50} calculated.

Mass spectroscopic analysis of the structure of purified compounds

The molecular weights of the purified compounds were determined using a high performance benchtop quadrupole trap atmospheric pressure chemical ionization mass spectrometry (APCI-MS; Thermo Fisher Scientific, MA, USA). The ion source was with a scan range of m/z 70 to 1050 and spray voltage of 5000 V, using nitrogen as the dry gas with a flow rate of 45 L/min.

RESULTS AND DISCUSSIONS

^{13}C-NMR Spectral Analysis for the DHP-G and DHP-GS

The ^{13}C-NMR spectra of the DHP-G and DHP-GS are shown in Figs. 4 and 5, respectively. The possible substructures are shown in Fig. 6. In Fig. 4, a weak α-CHO signal peak at 190.9 ppm (No. 1) was observed, indicating that a small amount of oxidation occurred during the DHP-G polymerization (Xie *et al*. 2000). The aliphatic carboxylic acid signal at 172.2 ppm (No. 2) showed that the γ-position had been oxidized to form cinnamic acid. Signals from 149.8 to 147.0 ppm (No. 4 to 8) were assigned to aromatic carbons of the guaiacyl ring. The signal at 143.6 ppm (No. 9) was from C4 of the 5-5 structure. The signals near 130 ppm (No. 10 to 14) were mainly the Cα/Cβ signals

from C=C, indicating that some double bonds in the side chain were not involved in the dehydrogenation reaction. Signals from 76.7 to 74.8 ppm (No. 22 to 23) and at 67.2 ppm (No. 27) were mainly from Cα and Cγ in the β-5 structure. This finding was similar to those of previous studies (Lüdemann and Nimz 1973; McElroy and Lai 1988). Peaks at 85.1 ppm (No. 21), 70.2 ppm (No. 26), and 62.0 ppm (No. 29) were mainly from Cβ, Cα, and Cγ of the β-O-4 structure, respectively (Harman-Ware *et al*. 2017). The signal at 63.5 ppm (No. 28) was from Cα of the β-1 structure. The peak at 53.5 ppm (No. 31) was assigned to Cβ of the β-β structure. The peak intensities indicated the content of β-5 and β-O-4 in the DHP-G was considerably higher than that of other substructures.

The ^{13}C-NMR spectra of the DHP-GS (Fig. 5) was similar to that of the DHP-G (Fig. 4), except for the signals that arose from the syringyl units. At low field chemical shifts of 191.3 ppm (No. 1') and 172.3 ppm (No. 2'), there were peaks corresponding to the C=O groups of the aromatic aldehyde and γ-position of ferulic acid, respectively (Holtman *et al*. 2004; Hage *et al*. 2009). The signal at 152.8 ppm (No. 4') was assigned to C3 and C5 on the etherified syringyl unit (Choi and Faix 2011). The resonances at 143.8 ppm (No. 7') and 129.1 ppm (No. 8') corresponded to C4 and C1 of the 5-5 structure, respectively. The peaks at 76.9 ppm (No. 16') and 67.3 ppm (No. 20') corresponded to Cα and Cγ of the β-5 structure, respectively. The peaks at 85.3 ppm (No. 15'), 71.0 ppm (No. 18'), and 61.8 ppm (No. 22') arose from the Cβ, Cα, and Cγ signals of the β-O-4 structure, respectively. The weak signal at 63.0 ppm (No. 21') corresponded to Cα of the β-1 structure. The peak at 45.2 ppm (No. 26') illustrated that some β-β structures were present. These results indicated that the DHP-GS also contained substructures, such as 5-5, β-O-4, β-5, β-1, and β-β, of which β-O-4 and β-5 were dominant.

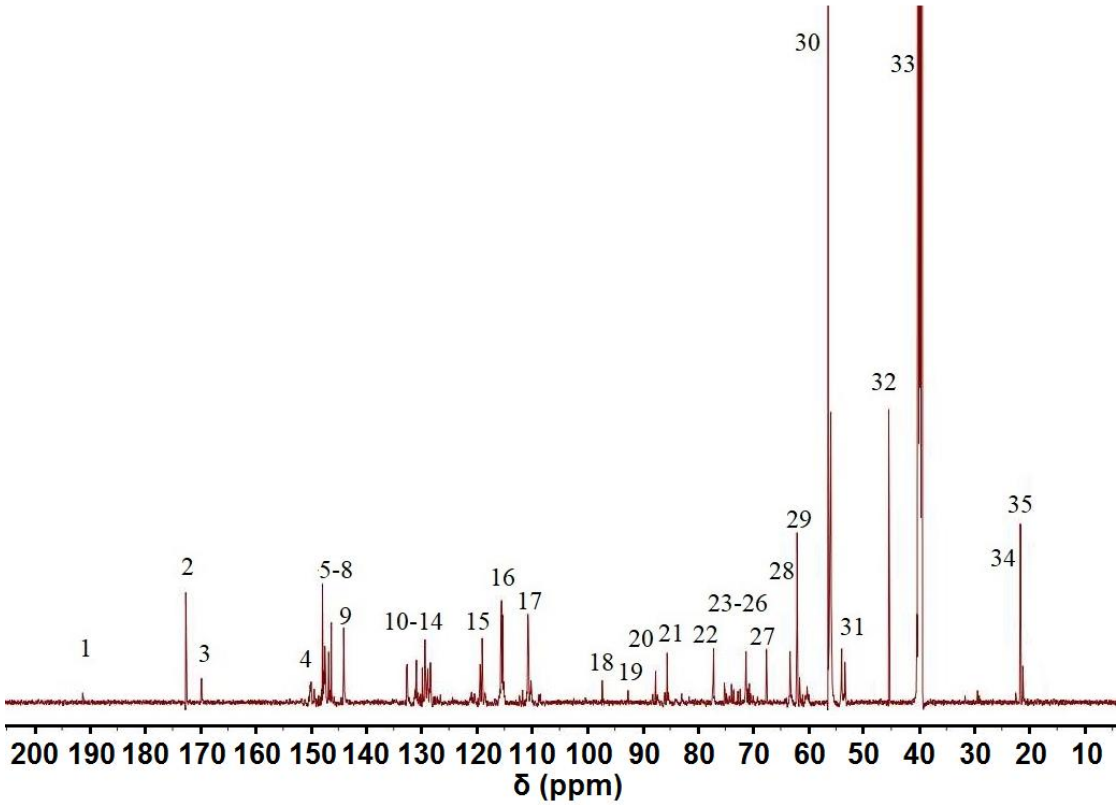

Fig. 4.^{13}C-NMR spectrum of the DHP-G

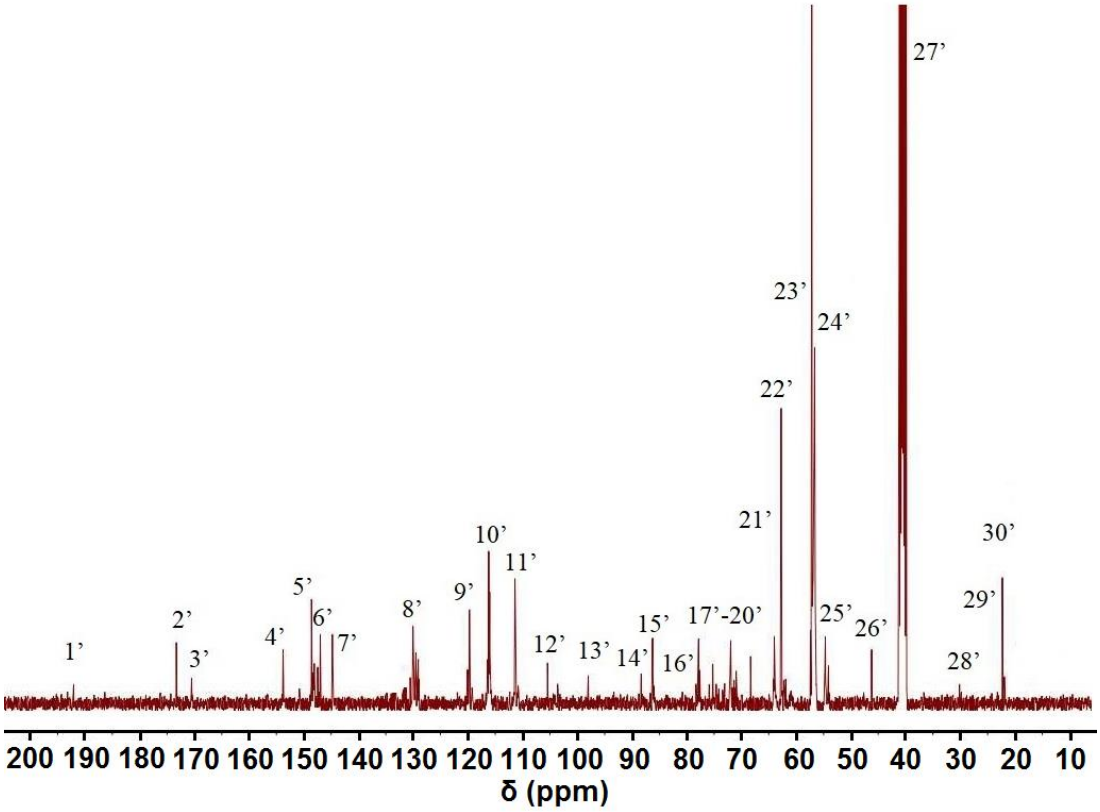

Fig. 5. ^{13}C-NMR spectrum of the DHP-GS

Molecular Weight Analyses of the DHP Fractions

To understand the degree of polymerization of the DHP fractions, the weight of average molecular weight (M_w) and number of average molecular weight (M_n) of each DHP fraction were determined. As shown in Table 1, the molecular weight of the four DHP-G fractions was much lower than that of naturally extracted lignin as milled wood lignin (MWL) according to the result of Huang *et al*. (2011).According to the molecular weight of coniferyl alcohol, *i.e*. 180 g/ mol, it was speculated that the dimer structure was dominant in F_{12} and F_{22}.

Table 1. Molecular Weight of the DHP Fractions

DHP Fractions	M_w	M_n
F_{11}	289	192
F_{12}	619	387
F_{13}	1527	988
F_{14}	2846	1923
F_{21}	293	181
F_{22}	677	462
F_{23}	1478	860
F_{24}	2642	1794

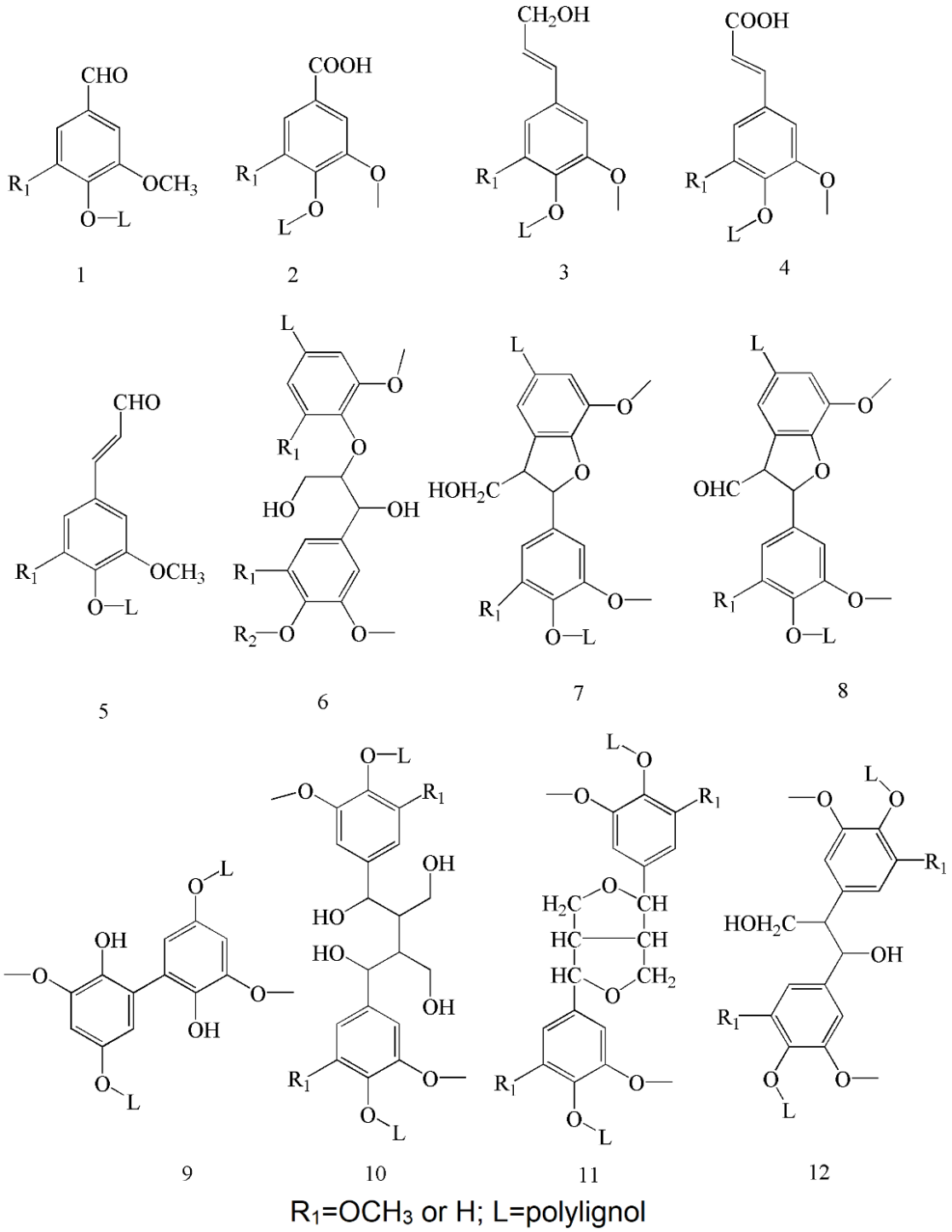

Fig. 6. Main substructures in the DHP-G and DHP-GS

Determination of Anticancer Activities of the DHP Fractions

The anticancer activities of the DHP fractions and the two lignin precursors are shown in Figs.7 and 8, and Table 2. The relationship between the sample concentration

and inhibitory rates were shown in log-fitting curves. Every fraction of DHP had a certain inhibitory effect on the Hela cervical cancer cells.

The inhibitory properties of two kinds of ether-soluble fractions, F_{12} and F_{22}, were relatively strong, with IC_{50} values of 81.60±9.30μg/mL and 103.24±14.09μg/mL, respectively. This also meant that the ether-soluble fraction from the DHP-G was more active than that from the DHP-GS. However, the IC_{50} values of coniferin and syringin were as high as 3844.75±86.51 μg/mL and 4410.96±106.94μg/mL, respectively, indicating that the activities of the two lignin precursors were low. As compared with the commercial anticancer drugs from plant as paclitaxel with IC_{50} of 7.08μM (6.04μg/mL) to cervical cancer (Yilmaz *et al*. 2016), the IC_{50} of the coniferin and the syringin was too high to be applied as drugs in anticancer purpose.

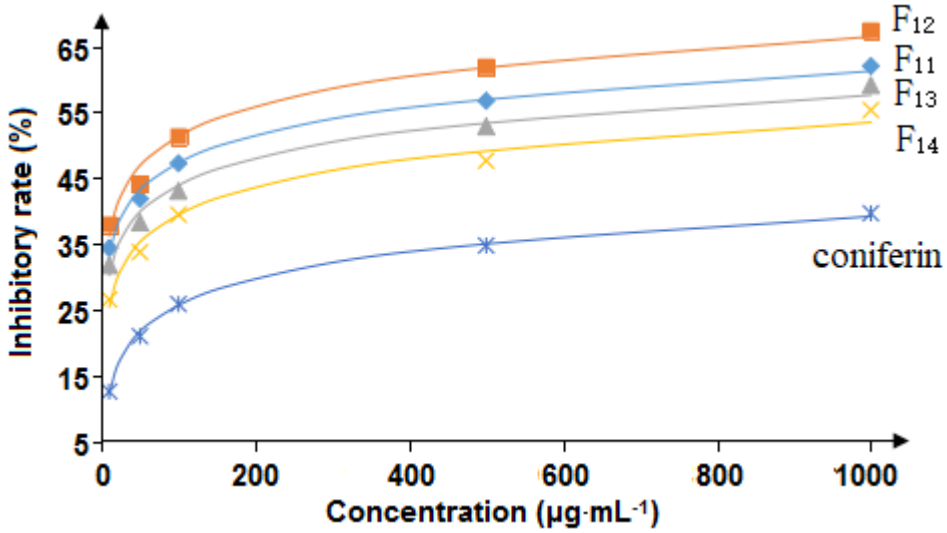

Fig. 7. The relationship between the concentrations of F_{11}, F_{12}, F_{13}, F_{14}, and coniferin and the inhibitory rates on cervical cancer cells

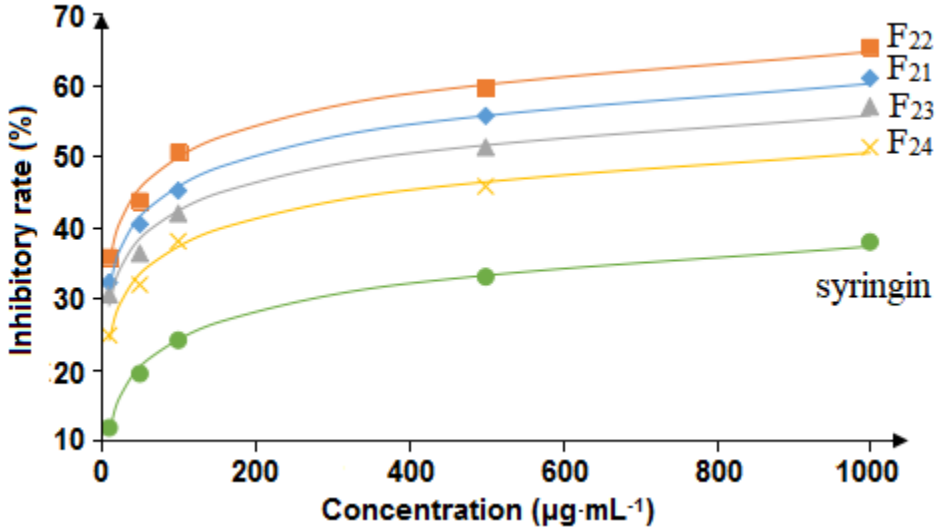

Fig. 8. The relationship between the concentrations of F_{21}, F_{22}, F_{23}, F_{24}, and syringin and the inhibitory rates on cervical cancer cells

Table 2. Inhibitory Effect of the DHP Fractions on the Hela Cervical Cancer Cells

DHP Fractions and precursors	IC_{50} (μg/mL)
F_{11}	157.67 ± 15.24
F_{12}	81.60 ± 9.30
F_{13}	282.64 ± 36.48
F_{14}	559.98 ± 57.33
F_{21}	201.08 ± 29.21
F_{22}	103.24 ± 14.09
F_{23}	378.73 ± 30.78
F_{24}	878.57 ± 36.72
Coniferin	3484.75 ± 86.51
Syringin	4410.96 ± 106.94

Anticancer Activity Analyses of the Purified DHP Compounds

Results from the anticancer experiment with purified compounds G_1 to G_5 and GS_1 to GS_5 are shown in Figs.9 and 10, and Table 3. It was found that only compounds G_1, G_2, GS_1, and GS_2 had low IC_{50} values on the Hela cervical cancer cells of 15.1±2.3, 40.5±7.6, 30.8±5.4, and 87.8±9.2 μg/mL, respectively. Of these, G_1 had the greatest inhibitory effect on growth, although its IC_{50} value on Hela cervical cancer cells was a little higher than that of paclitaxel (Yilmaz *et al*. 2016). However, because the IC_{50} value of the original F_{12} fraction was only 81.60±9.30μg/mL, these results further indicated G_1 and G_2 can be the most active compounds and play an important role in the efficacy of F_{12}. Similarly, the active anticancer substances in F_{22} were mainly GS_1 and GS_2, with IC_{50} values of 30.8±5.4 and 87.8±9.2μg/mL, respectively.

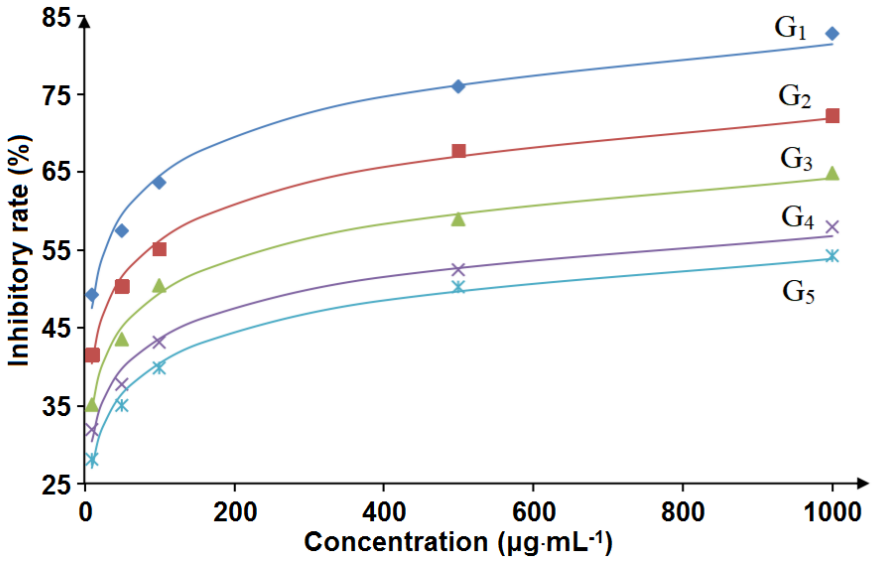

Fig. 9. Relationship between inhibitory rate and concentration of the purified compounds G_1 to G_5 on the Hela cervical cancer cells

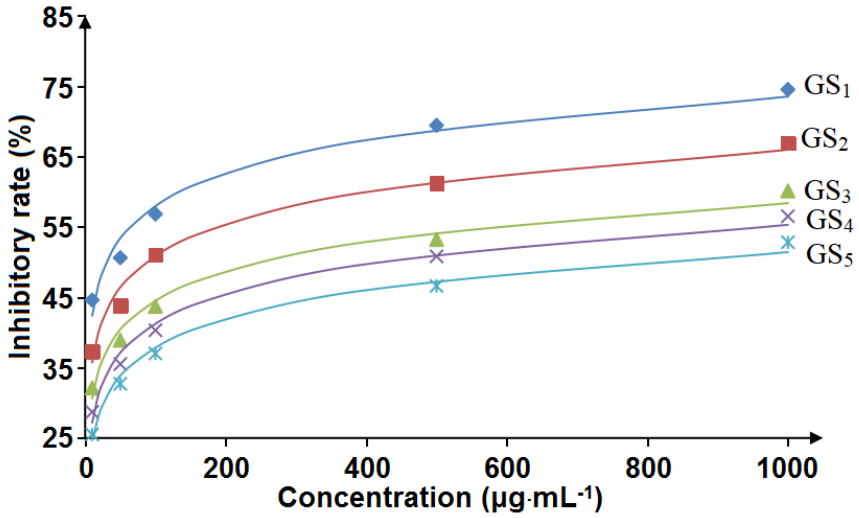

Fig. 10. Relationship between inhibitory rate and concentration of the purified compounds GS_1 to GS_5 on the Hela cells

Table 3. Inhibitory Effects of the Purified DHP Compounds on the Hela Cervical Cancer Cells

DHP compounds	IC_{50} (μg/mL)
G_1	15.1 ± 2.3
G_2	40.5 ± 7.6
G_3	110.7 ± 12.3
G_4	311.2 ± 18.2
G_5	515.5 ± 23.5
GS_1	30.8 ± 5.4
GS_2	87.8 ± 9.2
GS_3	251.9 ± 13.5
GS_4	420.3 ± 16.1
GS_5	756.3 ± 31.8

Structural Analyses of the Active Anticancer Compounds Isolated from the DHP-G and DHP-GS

Atmospheric pressure chemical ionization mass spectrometry (APCI-MS) is widely used to analyze weakly polar small-molecule polymers, with remarkable advantages in speed, specificity, and sensitivity over other methods. Mass spectrometry has now become one of the most important instruments in the analysis of lignin structures (Evtuguin and Amado 2003; Reale *et al*. 2004; Yang *et al*. 2010).

Molecular weight information for G_1 is shown in Fig.11. It was found that the molecular ion signal of G_1 appeared at *m/z*357.133. The fragment peak at *m/z*149.023 was formed by the γ-position carbon ionization in the side chain of coniferyl monomer. There was a structural signal peak formed by the cleavage of the γ-hydroxyl group at *m/z* 163.039. The ion signal peak at m/z 279.159 was a dimer of the β-5 structure. The fragment peak at *m/z*341.138 was from β-5, γ-CH_2^+. From the analyses of fragment peaks, it was proposed that the G_1 molecular ion at *m/z*357.133 was a G-type dimer (β-5, γ-CH_2OH, γ'-CH_2OH) (Fig.15, G_1), *i.e.*, *m/z* 4-[3-hydroxymethyl-5-(3-hydroxy-propenyl)-7-methoxy-2,3-dihydro-benzofuran-2-yl]-2-methoxy-phenol. This indicated that a coniferyl monomer with double bond in the side chain combined with the phenolic hydroxyl group of another monomer under laccase catalysis to form a β-5 structure.

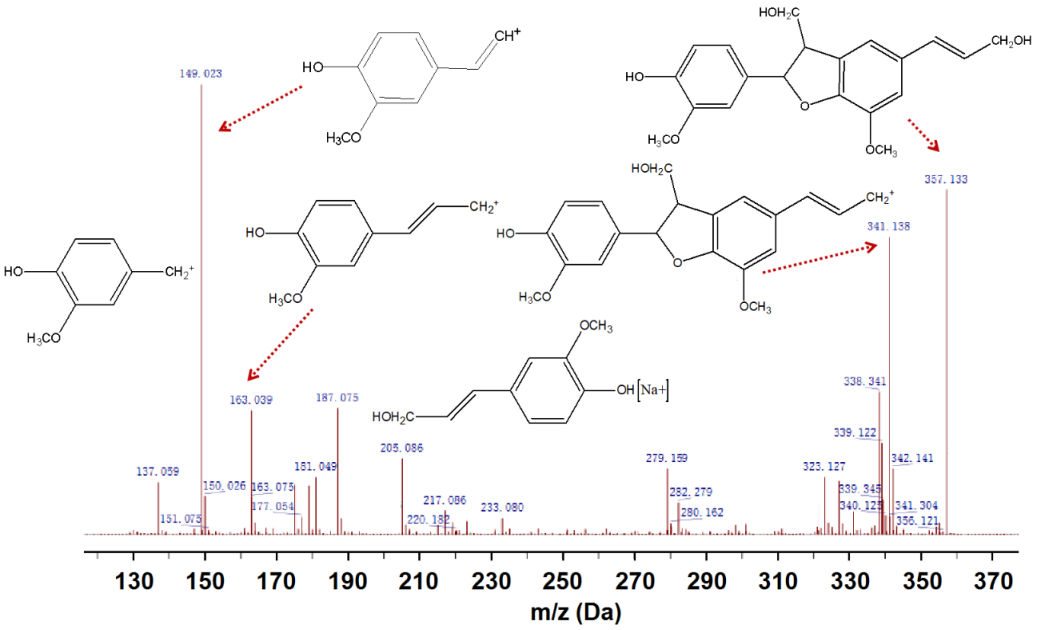

Fig. 11. Mass spectrum of the compound G_1
Legend: *m/z*137.059:2-Methoxy-4-methyl-phenol;*m/z*149.023: 2-Methoxy-4-vinylphenol;*m/z*163.039:2-Methoxy-4-propenyl-phenol;*m/z*205.086:4-(3-Hydroxy-propenyl)-2-methoxy-phenol[Na^+];*m/z*341.138: 4-(3-Hydroxymethyl-7-methoxy-5-propenyl-2,3-dihydro-benzofuran-2-yl)-2-methoxy-phenol;*m/z*357.133:4-[3-Hydroxymethyl-5-(3-hydroxy-propenyl)-7-methoxy-2,3-dihydro-benzofuran-2-yl]-2-methoxy-phenol

The mass spectrum of G_2 is shown in Fig. 12. The signal peak at *m/z* 219.065 was formed by the breaking of the ether bond and carbon-carbon bond on the coumaran ring in the structure of phenylcoumaran. The signal at *m/z*314.177 was generated by the cleavage of the carbon-carbon double bond in the side chain of the β-5 dimer. The signal of *m/z*341.138 (β-5, γ-COOH) was strong, indicating that many monomers were polymerized by β-5 linkage, and the side chain was easily oxidized to a carboxylic acid structure. The parent ion of the fragment at *m/z*219.065 appeared at *m/z*357.133 and its structure was β-5, γ'-COOH. The signal of *m/z*392.287 was produced by β-5 (γ-CH_2OH, γ'-COOH) dimer capturing Na^+. The molecular ion peak of G_2 appeared at *m/z*564.221. According to the analysis of fragment peaks, it was assigned to 5-(2-Carboxy-vinyl)-2'-(4-hydroxy-3-methoxy-phenyl)-3-hydroxymethyl-7,7'-dimethoxy-2,3,2',3'-tetrahydro-[2,5']bibenzofur-anyl-3'-carboxylic acid, which indicated the structure of G_2 to be a G-type trimer [(β-5)(β-5), γ-COOH, γ'-CH_2OH, γ''-COOH] (Fig. 15, G_2). The fragment structure trimer [(β-5)(β-5), γ-COOH, γ'-CH_2OH, β''-CH^+] at *m/z*519.201 also confirmed the G_2 structure.

Molecular weight information for GS_1 is shown in Fig.13. The signal of *m/z* 205.086 was a typical fragment of the β-5 type dimer after coumaran ring breaking. The signal at *m/z*233.080 was formed by the capture of Na^+ by the sinapyl alcohol monomer. The ion peak at *m/z*387.143 revealed the structure of 4-[3-hydroxymethyl-5-(3-hydroxy-propenyl)-7-methoxy-2,3-dihydro-benzofuran-2-yl]-2,6-dimethoxy-phenol, which was a β-5 GS-type dimer (Fig. 15, GS_1). Further analyses of fragment ion peaks at *m/z*149.023, 187.075, and 205.086 confirmed signal at *m/z*387.143 to be a dimer [(β-5), γ-CH_2OH, γ'-CH_2OH] formed by G-type and S-type monomers. The molecular weight difference

between *m/z*357.132 and *m/z*387.143 was 30, exactly the molecular weight of -CH_2OH, indicating that the γ position was relatively easily to be eliminated, and reassured the structure of GS_1.

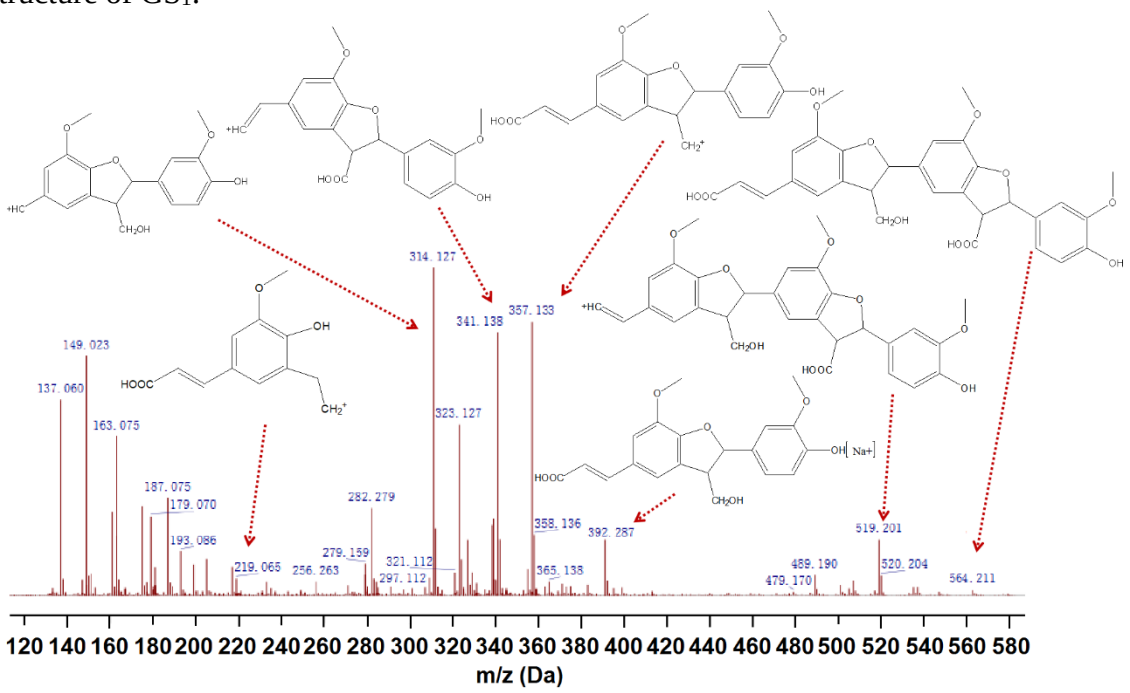

Fig. 12. Mass spectrum of the compound G_2
Legend: *m/z* 219.065: 3-(3-Ethyl-4-hydroxy-5-methoxy-phenyl)-acrylic acid; *m/z*314.127:4-(3-Hydroxymethyl-7-methoxy-5-methyl-2,3-dihydro-benzofuran-2-yl)-2-methoxy-phenol, (β-5, γ-OH);*m/z* 341.138: 2-(4-Hydroxy-3-methoxy-phenyl)-7-methoxy-5-vinyl-2,3-dihydro-benzofuran-3-carboxylic acid;357.*m/z* 133:3-[2-(4-Hydroxy-3-methoxy-phenyl)-7-methoxy-3-methyl-2,3-dihydro-benzofuran-5-yl]-acrylic acid; *m/z* 392.287:3-[2-(4-Hydroxy-3-methoxy-phenyl)-3-hydroxymethyl-7-methoxy-2,3-dihydro-benzofuran-5-yl]-acrylic acid[Na^+]; *m/z* 519.201:2'-(4-Hydroxy-3-methoxy-phenyl)-3-hydroxymethyl-7,7'-dimethoxy-5-vinyl-2,3,2',3'-tetrahydro-[2,5']bibenzofuranyl-3'-carboxylic acid; *m/z* 564.211:5-(2-Carboxy-vinyl)-2'-(4-hydroxy-3-methoxy-phenyl)-3-hydroxymethyl-7,7'-dimethoxy-2,3,2',3'-tetrahydro-[2,5']bibenzofuranyl-3'-carboxylic acid.

The GS_2 was a compound eluted from the preparative column chromatography with acetone/n-hexane mixture (3:2 v/v) as the mobile phase. The GS_2 had a higher degree of polymerization than the GS_1. The mass spectrum of GS_2 is shown in Fig.14. The signal peaks with strong abundance were mainly found at *m/z*137.059, *m/z*163.075, *m/z*311.127, *m/z*323.127, and *m/z*341.138. The signal at *m/z*311.127 was a fragment produced by the γ-CH_2OH cleavage in the β-O-4 dimer. An ion peak appeared at *m/z*341.155 was a fragment signal generated by the ionization of the side chain hydroxyl group of the G-type [(β-O-4), γ-CH_2OH, γ'-CH_2OH] dimer. A molecular ion observed at *m/z*415.138 was a fragment produced by the (β-O-4)(β-5) trimer. Analyses of fragment ion peaks (Izumi and Kuroda 1997; Kang *et al.* 2012) at *m/z*137.059, 210.065, 311.127, 341.138, 415.138, and the molecular ion peak at *m/z*568.138 indicated that these signals were from the 4-(5-{3-hydroxy-2-[4-(3-hydroxy-propenyl)-2-methoxy-phenoxy]-propyl}-3-hydroxymethyl-7-methoxy-2,3-dihydro-benzofuran-2-yl)-2,6-dimethoxy-phenol, revealing the GS_2 structure to be a GS-type trimer [(β-O-4)(β-5), γ-CH_2OH, γ'-CH_2OH, γ''-CH_2OH] (Fig. 15, GS_2).

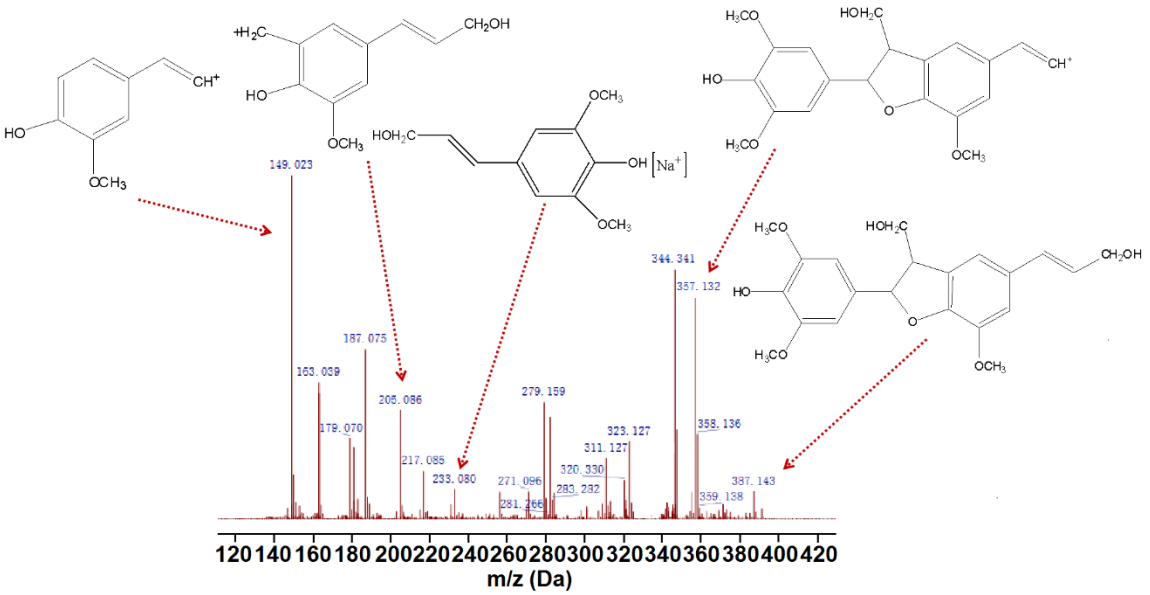

Fig. 13. Mass spectrum of the compound GS_1
Legend: *m/z*149.023: 2-Methoxy-4-vinyl-phenol; *m/z*187.075: 4-(3-Hydroxy-propenyl)-2-methoxy-6-methyl-phenol;*m/z*205.086: 4-(3-Hydroxy-propenyl)-2-methoxy-6-methyl-phenol; *m/z* 233.080: 4-(3-Hydroxy-propenyl)-2,6-dimethoxy-phenol [Na^+];*m/z*357.132: 4-(3-Hydroxymethyl-7-methoxy-5-vinyl-2,3-dihydro-benzofuran-2-yl)-2,6-dimethoxy-phenol; *m/z*387.143: 4-[3-Hydroxymethyl-5-(3-hydroxy-propenyl)-7-methoxy-2,3-dihydro-benzofuran-2-yl]-2,6-dimethoxy-phenol.

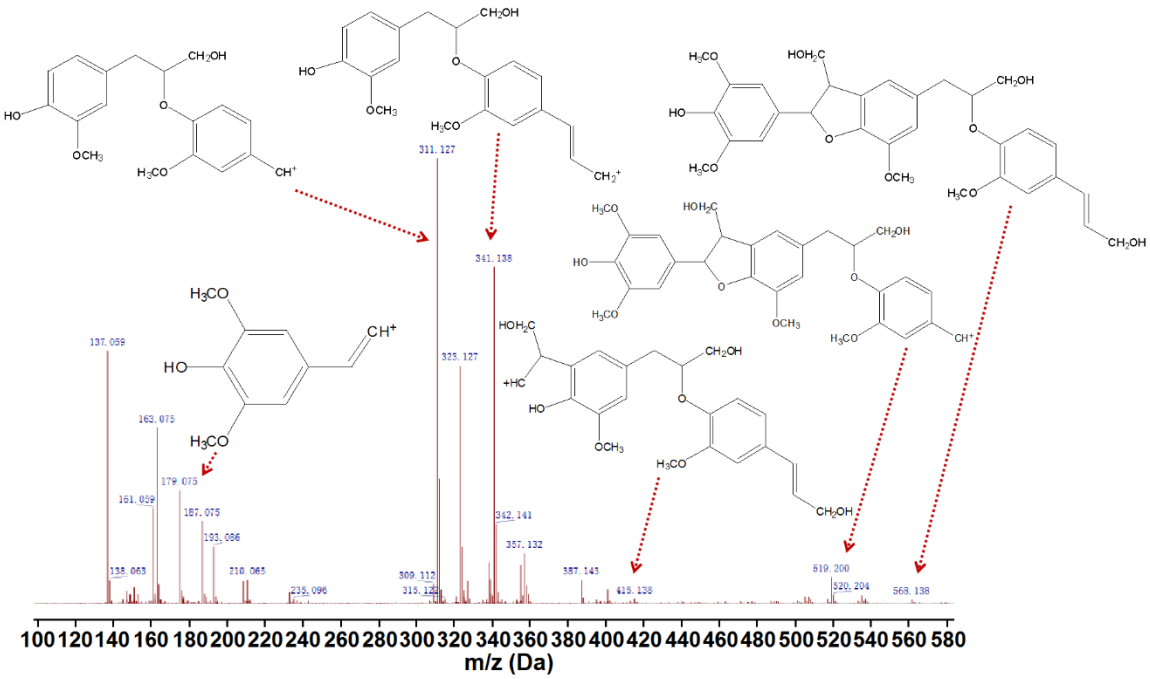

Fig. 14. Mass spectrum of the compound GS_2
Legend: *m/z*137.059: 2-Methoxy-4-methyl-phenol;*m/z*179.075: 2-Methoxy-4-vinyl-phenol; *m/z*210.065: 4-(3-Hydroxy-propenyl)-2-methoxy-phenol;*m/z*311.127: 4-[3-Hydroxy-2-(2-methoxy-4-methyl-phenoxy)-propyl]-2-methoxy-phenol; *m/z*341.138: 4-[3-Hydroxy-2-(2-methoxy-4-propenyl-phenoxy)-propyl]-2-methoxy-phenol; *m/z*415.138: 4-{3-Hydroxy-2-[4-(3-hydroxy-propenyl)-2-methoxy-phenoxy]-propyl}-2-(2-hydroxy-1-methyl-ethyl)-6-methoxy-phenol;*m/z*568.138: 4-(5-{3-Hydroxy-2-[4-(3-hydroxy-propenyl)-2-methoxy-phenoxy]-propyl}-3-hydroxymethyl-7-methoxy-2,3-dihydro-benzofuran-2-yl)-2,6-dimethoxy-phenol

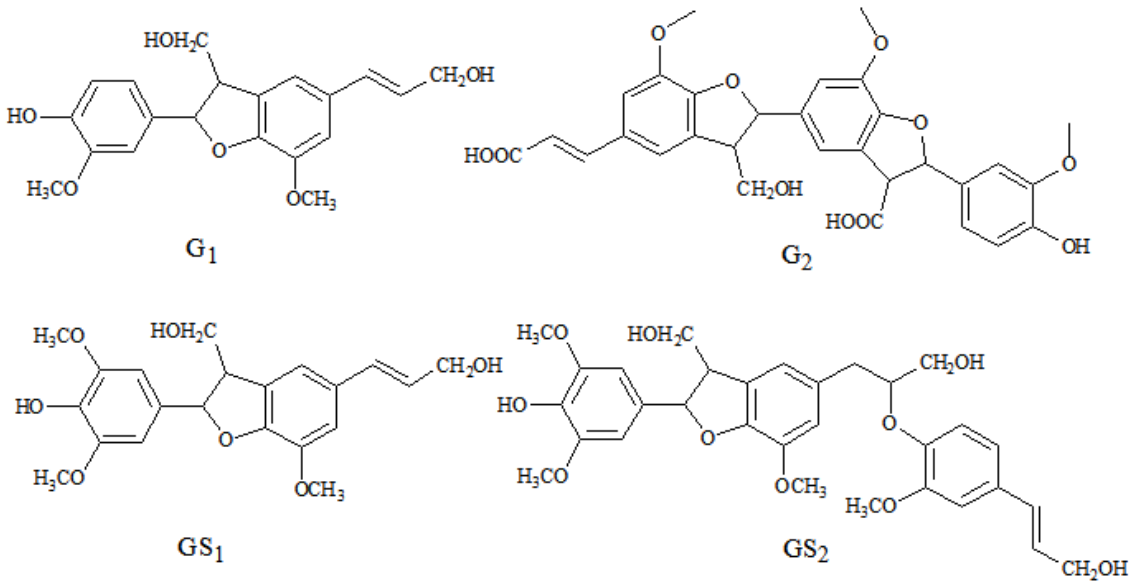

Fig. 15. Chemical structures of the compound G_1, G_2, GS_1, and GS_2

As shown in Fig. 15, APCI-MS analysis indicated that the chemical structures of G_1, G_2, GS_1, andGS_2 were as follows: G_1, β-5 G-type dimer; G_2, (β-5) (β-5) G-type trimer; GS_1, β-5 GS-type dimer; and GS_2, (β-O-4) (β-5) GS-type trimer. Mass spectroscopic analysis revealed that the compound G_1 was a pure G-type dimer [(β-5), γ-CH_2OH, γ'-CH_2OH]. However, the compound GS_1 was a GS-type dimer [(β-O-4) (β-5), γ-CH_2OH, γ'-CH_2OH, γ"-CH_2OH]. The structural difference was only due to the methoxyl group at the 5-position of the syringyl units.

The difference in biological activity between compounds G_1 and GS_1 was obvious. Although the anticancer activities of these two substances were relatively high, the stronger biological activity of the compound G_1 indicated that the methoxyl group on the syringyl units of GS_1 weakened the anticancer activity of oligomeric DHP. Compared with GS_1, it was found that the chemical structure of GS_2 differed in the increased β-O-4 linkages, but its anticancer activity decreased by more than half, indicating that the β-O-4 structure did not contribute to the anticancer activity of DHP. As compared with the IC_{50} value of GS_2, the IC_{50} of G_2 was much lower as shown in Table 3. This revealed the anticancer activity of G_2 was stronger than that of GS_2. It was illustrated that the carboxyl group did contribute to the anticancer activity of DHP. Dziedzicand Hudson (1984)also found that the introduction of a carboxyl group into the pyrogallol molecule brings about a great increase in antioxidant activity. It was supposed that the unsaturated side chain contributed to the radical-induced lignification of the cell membrane of the Hela cervical cancer cells and inhibition of mass exchange. In addition, there is also the possibility that the phenylcoumaran (β-5) structure of the oligomeric DHP components destroyed the cell membrane of cervical cancer cells.

CONCLUSIONS

1. The DHP-G and DHP-GS were synthesized by laccase catalytic dehydrogenation polymerization. The ^{13}C-NMR spectra indicated that both DHPs contained 5-5, β-O-4, β-1, β-5, and β-β substructures.
2. The ether-soluble fractions F_{12} and F_{22} had good inhibitory activity against cervical cancer Hela cells. Determination of anticancer effects of the compounds isolated from these DHP fractions by preparative column chromatography indicated G_1, G_2, GS_1, and GS_2 had strong anticancer activity.
3. According to APCI-MS measurements, it was found that the compound G_1 was a (β-5) G-type dimer, whereas the compound G_2 was a (β-5) (β-5) G-type trimer. It was also found that the compound GS_1 was a (β-5) GS-type dimer and the GS_2 a (β-O-4) (β-5) GS-type trimer.
4. From the analysis of the structure-effect relationship, it was found that increased methoxyl groups of the syringyl units weakened the anticancer activity of oligomeric DHP. Moreover, the increase of β-O-4 linkages did not contribute substantially to the anticancer activity. It was also found that the carboxyl groups contributed to the anticancer activity of DHP.

ACKNOWLEDGMENTS

The authors are grateful for the support of the National Natural Science Foundation of China (grant No. 21878070).

REFERENCES CITED

Barapatre, A., Meena, A. S., Mekala, S., Das, A., and Jha, H. (2016). "*In vitro* evaluation of antioxidant and cytotoxic activities of lignin fractions extracted from *Acacia nilotica*," *International Journal of Biological Macromolecules* 86, 443-453. DOI: 10.1016/j.ijbiomac.2016.01.109

Chen, X. K., Zhao, H. K., Wu, H. F., Ye, Z. Z., and Xie, Y. M. (2018). "Preparation and antioxidant properties of dehydrogenation polymer of isoeugenol," *Chemistry and Industry of Forest Products* 38(1), 87-92. DOI: 10.3969/j.issn.0253-2417.2018.01.013

Choi, J. W., and Faix, O. (2011). "NMR study on residual lignins isolated from chemical pulps of beech wood by enzymatic hydrolysis," *Journal of Industrial and Engineering Chemistry* 17(1), 25-28. DOI: 10.1016/j.jiec.2010.10.004

Dai, J., and Mumper, R J. (2010). "Plant phenolics: Extraction, analysis and their antioxidant and anticancer properties," *Molecules* 15(10), 7313-7352. DOI: 10.3390/ molecules15107313

Dziedzic, S. Z., and Hudson, B. J. (1984). "Phenolic acids and related compounds as antioxidants for edible oils," *Food Chemistry* 14(1), 45-51. DOI: 10.1016/0308-8146(84)90017-7

Evtuguin, D. V., and Amado, F. M. (2003). "Application of electrospray ionization mass spectrometry to the elucidation of the primary structure of lignin," *Macromolecular Bioscience* 3(7), 339-343.DOI: 10.1002/mabi.200350006

Freudenberg, K. (1952). "Die Entstehung des Lignins in der Pflanze [The emergence of lignin in the plant]," *Holzforschung* 6(2), 37-42. DOI: 10.1515/hfsg.1952.6.2.37

Gomes, C. A., Girão da Cruz, T., Andrade, J. L., Milhazes, N., Borges, F., and Marques, M. P. M. (2003). "Anticancer activity of phenolic acids of natural or synthetic origin: A structure-activity study," *Journal of Medicinal Chemistry* 46(25), 5395-5401. DOI: 10.1021/jm030956v10.1002/mabi.200350006

Guan, S. Y., Mlynár, J., and Sarkanen, S. (1997). "Dehydrogenative polymerization of conifery alcohol on macromolecular lignin templates," *Phytochemistry* 45(5), 911-918. DOI: 10.1016/S0031-9422(97)00077-0

Hage, E. R., Brosse, N., Chrusciel, L., Sanchez, C., Sannigrahi, P., and Ragauskas, A. (2009). "Characterization of milled wood lignin and ethanol organosolv lignin from miscanthus," *Polymer Degradation and Stability* 94(10), 1632-1638. DOI: 10.1016/j.polymdegradstab.2009.07.007

Harman-Ware, A. E., Happs, R. M., Davison, B. H., and Davis, M. F. (2017). "The effect of coumaryl alcohol incorporation on the structure and composition of lignin dehydrogenation polymers," *Biotechnology for Biofuels* 10(1), Article Number 281. DOI: 10.1186/s13068-017-0962-2

Holtman, K. M., Chang, H. M., and Kadla, J. F. (2004). "Solution-state nuclear magnetic resonance study of the similarities between milled wood lignin and cellulolytic enzyme lignin," *Journal of Agricultural and Food Chemistry* 52(4), 720-726. DOI: 10.1021/jf035084k

Huang, F., Singh, P. M., and Ragauskas, A. J. (2011). "Characterization of milled wood lignin (MWL) in loblolly pine stem wood, residue, and bark," *Journal of Agricultural and Food Chemistry* 59(24), 12910-12916. DOI: 10.1021/jf202701b

Izumi, A., and Kuroda, K. I. (1997). "Pyrolysis-mass spectrometry analysis of dehydrogenation lignin polymers with various syringyl/guaiacyl ratios," *Rapid Communications in Mass Spectrometry* 11(15), 1709-1715. DOI: 10.1002/(sici)1097-0231(19971015)11:15<1709::aid-rcm5>3.0.co;2-j

Jia, J., Qu, Y. C., Gao, Y., Yuan, Y. P., Wang, K. K., Yang, F., Wu, G. F., and Li, Y. F. (2013). "Separation of lignin from pine-nut hull by the method of HBS and preparation of lignin-PEG-PAPI," *Applied Mechanics and Materials* 320, 429-434. DOI: 10.4028/www.scientific.net/AMM.320.429

Kang, S., Xiao, L., Meng, L., Zhang, X., and Sun, R. (2012). "Isolation and structural characterization of lignin from cotton stalk treated in an ammonia hydrothermal system," *International Journal of Molecular Sciences* 13(11), 15209-15226. DOI: 10.3390/ijms131115209

Lüdemann, H. D., and Nimz, H. (1973). "Carbon-13 nuclear magnetic resonance spectra of lignins," *Biochemical and Biophysical Research Communications* 52(4), 1162-1169. DOI:10.1016/0006-291X(73)90622-0

Mathi, P., Nikhil, K., Ambatipudi, N., Roy, P., Bokka, V. R., and Botlagunta, M. (2014). "*In-vitro* and *in-silico* characterization of *Sophora interrupta* plant extract as an anticancer activity," *Bioinformation* 10(3), 144-151. DOI: 10.6026/97320630010144

Mathi, P., Das, S., Nikhil, K., Roy, P., Yerra, S., Ravada, S. R., Bokka, V. R., and Botlagunta, M. (2015). "Isolation and characterization of the anticancer compound

piceatannol from *Sophora interrupta* Bedd," *International Journal of Preventive Medicine* 6, Article Number 101. DOI: 10.4103/2008-7802.167181

McCarthy, J. L., and Islam, A. (1999). "Lignin chemistry, technology, and utilization: A brief history," in: *Lignin Historical Biological and Material Perspectives, ACS Symposium Series*, Volume 742, W. G. Glasser, R. A. Northey, T. P. Schultz (eds.), American Chemical Society, Washington DC, USA, pp. 2-99. DOI: 10.1021/bk-2000-0742.ch001

McElroy, R. D., and Lai, K. (1988). "Fractionation-purification, IR, 1H 13C NMR spectral and property studies of an industrial based sludge lignin," *Journal of Wood Chemistry and Technology* 8(3), 361-378. DOI: 10.1080/02773818808070690

Niedzwiecki, A., Roomi, M., Kalinovsky, T., and Rath, M. (2016). "Anticancer efficacy of polyphenols and their combinations," *Nutrients* 8(9), 1-17. DOI: 10.3390/nu80905 52

Obst, J. R., and Kirk, T. K. (1988). "Isolation of lignin," *Methods in Enzymology* 161(1), 3-12. DOI: 10.1016/0076-6879(88)61003-2

Quideau, S., Deffieux, D., Douat-Casassus, C., and Pouysegu, L. (2011). "Plant polyphenols: chemical properties, biological activities, and synthesis,"*AngewandteChemie International Edition* 50(3), 586-621. DOI: 10.1002/anie.201000044

Reale, S., Di Tullio, A., Spreti, N., and De Angelis, F. (2004). "Mass spectrometry in the biosynthetic and structural investigation of lignins," *Mass Spectrometry Reviews* 23(2), 87-126. DOI: 10.1002/mas.10072

Sakagami, H., Hashimoto, K., Suzuki, F., Ogiwara, T., Satoh, K., Ito, H., Hatano, T., Takashi, Y., and Fujisawa, S. I. (2005). "Molecular requirements of lignin-carbohydrate complexes for expression of unique biological activities," *Phytochemistry* 66(17), 2108-2120. DOI: 10.1016/j.phytochem.2005.05.013

Tan, C., Kong, L., Li, X., Li, W., and Li, N. (2011). "Isolation and analysis of a new phytoecdysteroid from *Cyanotis arachnoidea* CB Clarke," *Chinese Journal of Chromatography* 29(9), 937-941. DOI: 10.3724/SP.J.1123.2011.00937

Vinardell, M., and Mitjans, M. (2017). "Lignins and their derivatives with beneficial effects on human health," *International Journal of Molecular Sciences* 18(6), 1-15. DOI: 10.3390/ijms18061219

Van, M. J., Kaspers, G. J., and Cloos, J. (2011). "Cell sensitivity assays: The MTT assay," in: *Cancer Cell Culture*, S. P. Langdon (ed.), Humana Press, Totowa, NJ, USA, pp.165-169. DOI: 10.1007/978-1-61779-080-5_20

Wang, K., Xu, F., and Sun, R. (2010). "Molecular characteristics of kraft-AQ pulping lignin fractionated by sequential organic solvent extraction," *International Journal of Molecular Sciences* 11(8), 2988-3001. DOI: 10.3390/ijms11082988

Xiang, Y. (2015). "Introduction of column chromatography for mixture separation," *Chinese Journal of Chemical Education* 2015(17), 1-3. DOI: 10.13884/j.1003-3807hxjy.2014090136

Xie, Y. (1991). "Selective carbon 13-enrichment of side chain carbons of ginkgo lignin traced by carbon 13 nuclear magnetic resonance," *Mokuzai Gakkaishi* 37, 935-941.

Xie, Y., Yasuda, S., and Terashima, N. (1994a). "Selective carbon 13-enrichment of side chain carbons of oleander lignin traced by carbon 13 nuclear magnetic resonance," *Journal of the Japan Wood Research Society* 40(2), 191-198.

Xie, Y., Robert, D. R., and Terashima, N. (1994b). "Selective carbon 13 enrichment of side chain carbons of ginkgo lignin traced by carbon 13 nuclear magnetic resonance," *Journal of the Japan Wood Research Society* 32(2), 243-249.

Xie, Y., Chen, X., Jiang, C., Wu, H., and Ye, Z. (2019). "Preparation of oligomeric dehydrogenation polymer and characterization of its antibacterial properties," *BioResources* 14(2), 2842-2860.DOI: 10.15376/biores.14.2.2842-2860

Xie, Y., Yasuda, S., Wu, H., and Liu, H. (2000). "Analysis of the structure of lignin-carbohydrate complexes by the specific 13 C tracer method," *Journal of Wood Science* 46(2), 130-136.DOI: 10.1007/BF00777359

Yang, Q., Wu, S., Lou, R., and Lv, G. (2010). "Analysis of wheat straw lignin by thermogravimetry and pyrolysis–gas chromatography/mass spectrometry," *Journal of Analytical and Applied Pyrolysis* 87(1), 65-69.DOI: 10.1016/j.jaap.2009.10.006

Ye, Z. Z., Xie, Y. M., Wu, C. X., Wang, P., and Le, X. (2016). "Dehydrogenation polymerization of isoeugenol and formation of lignin-carbohydrate complexes with presence of polysaccharide," *Chemistry and Industry of Forest Products* 36(2), 45-50.DOI: 10.3969/j.issn.0253-2417.2016.02.007

Yilmaz, A., Alp, E., Onen, H. I., and Menevse, S. (2016). "Reduced BCL2 and CCND1 mRNA expression in human cervical cancer HeLa cells treated with a combination of everolimus and paclitaxel," *Contemporary Oncology* 20(1), 28-32.DOI: 10.5114/wo.2016.58498

Article submitted: October 11, 2019; Peer review completed: January 14, 2020; Revised version received and accepted: January 18, 2020; Published: January 27, 2020.
DOI: 10.15376/biores.15.1.1791-1809